Available online at www.sciencedirect.com
SCIENCE DIRECT®
International Journal of Mass Spectrometry 228 (2003) 629–646
International Journal of Mass Spectrometry
www.elsevier.com/locate/ijms

Investigations of the gas-phase reactivity of Cu^+ and Ag^+ glycine complexes towards CO, D_2O and NH_3

Doina Caraiman[1], Tamer Shoeib[2], K.W. Michael Siu, Alan C. Hopkinson, Diethard K. Bohme*

Centre for Research in Mass Spectrometry and Centre for Research in Earth and Space Science, Department of Chemistry, York University, 4700 Keele Street, Toronto, Ont., Canada M3J 1P3

Received 26 November 2002; accepted 20 March 2003

Dedicated to Helmut Schwarz on the occasion of his 60th birthday and in recognition of his many splendid contributions to gas-phase ion chemistry.

Abstract

The room-temperature reactivities of complexes of Cu^+ and Ag^+ with glycine have been investigated using an inductively coupled plasma-selected ion flow tube (ICP-SIFT)/multicollision-induced dissociation (CID) tandem mass spectrometer. These complexes were produced in a flow tube, collisionally thermalized and then allowed to react with CO, D_2O or NH_3. The measured reactivities of the $CuGly^+$ and $AgGly^+$ complexes have been compared with those of the bare metal cations towards the same neutral reagents. All observed reactions resulted in adduct formation, with helium buffer gas presumably acting as a stabilizing agent. Reaction rate enhancements of up to three orders of magnitude and lower extents of ligation were the main characteristics of the reactions initiated by the metal cation–glycine adducts as compared with those initiated by the bare metal cations. The kinetic information combined with equilibrium analyses and CID results suggest that, irrespective of the reagent, ligation to $CuGly^+$ is stronger than to $AgGly^+$ and, in both instances, ligation of carbon monoxide and water has comparable strengths, while much stronger coordination is achieved with ammonia. The structures of the complexes have been investigated computationally using density functional theory (DFT) at the B3LYP level employing the DZVP basis set. Optimized structures and the free energy changes associated with ligation have been computed. A good correlation was obtained between the experimental reaction efficiencies and the calculated free energies of bonding. Also, results are presented for the potential energy surfaces for the conversion of the "charge solvated" forms into the "metal salt" forms of $CuGly^+$ and $AgGly^+$ and of their adducts with CO or NH_3. The computations indicate a modest catalytic effect of the CO and NH_3 on this conversion.

Keywords: Metal ions; Glycine; Charge solvated; Metal salts; Ligation

1. Introduction

Gas-phase transition metal ion chemistry has experienced explosive growth in the recent past [1–3] and has been stimulated in part by the importance of transition metal ions in a wide variety of fields including catalysis, organometallic reactions and especially in

* Corresponding author. Tel.: +1-416-736-2100x66188; fax: +1-416-736-5936.
E-mail address: dkbohmme@science.yorku.ca (D.K. Bohme).
[1] Present address: MDS SCIEX, 71 Four Valley Dr., Concord, Ont., Canada L4K 4V8.
[2] Present address: Thermofinnigan, 355 River Oaks Parkway, San Jose, CA 95134, USA.

1387-3806/$ – see front matter © 2003 Elsevier Science B.V. All rights reserved.
doi:10.1016/S1387-3806(03)00210-0

biochemistry where metal ions can be very influential in determining the three-dimensional structures of nucleic acids [4–7]. For many proteins, a variety of metal ions are required to interact with the appropriate peptides in order for the latter to be able to carry out their regulatory or structural functions [8]. It is therefore important that we advance our understanding of the interactions of these metal ions with molecules of biological importance.

Transition metal ions, such as Cu^+, also play very important roles in biological processes such as oxidation, dioxygen transport and electron transfer [9–12]. Compounds containing Ag^+ are used as potent antibacterial agents [13] and also are among the most toxic towards bacteria and other microorganisms.

The tendency of a variety of metal ions to bind to peptides has been exploited in the field of mass spectrometry in which metal ions such as Li^+, Na^+, Cu^+ and Ag^+ have been used as ionizing agents for peptide sequencing [14–16]. Also, since amino acids are the basic constituents of proteins and can be used to model the reactivities of more complicated biological systems, their interactions with metal ions in the gas phase are topics of much current interest [17–19]. Gas-phase mass spectrometry experiments allow the study of the 'intrinsic' modes of binding governing metal–amino acid complexes.

Recently, the kinetic method has been used to obtain ladders of relative Cu^+ and Ag^+ affinities of almost all essential α-amino acids [20,21]. Theoretical studies also have investigated the interaction of Cu^+ and Ag^+ with amino acids, including the smallest one, glycine [22–25].

Here we investigate the reactivities of Cu^+ and Ag^+ complexed with glycine in the gas phase towards three neutral molecules that have biological relevance: carbon monoxide, water and ammonia. Measured rate coefficients and product ion distributions for the reactions of these metal–cation–glycine adducts are compared with those obtained for reactions of the bare metal cations with the same neutral reagents. The structures and energetics of the resulting product ions are investigated theoretically.

In the gas-phase glycine is known to exist in the neutral form ($H_2N–CH_2–COOH$) [26a–d] while in the solution phase the zwitterionic form ($H_3{}^+N–CH_2–COO^-$) is dominant [27]. Calculations have shown that the glycine zwitterion does not exhibit a potential minimum in the gas phase but that the interaction of a metal cation with glycine can stabilize the zwitterionic form [29a–d]. Here we investigate this stabilization and determine the difference in stability of the neutral and the zwitterionic form of glycine–metal cation complexes. The influence of a ligand such as CO or NH_3 was also considered in order to examine any catalytic effects these ligands might have on the interconversion between the two forms of these glycine–metal cation complexes.

2. Experimental

The experiments were performed with the newly configured inductively coupled plasma-selected ion flow tube (ICP-SIFT) tandem mass spectrometer [30]. The atomic metal cations Cu^+ and Ag^+ were generated in an argon plasma at 5500 K fed with a vaporized solution containing the metal. The ions produced were injected through a differentially-pumped sampling interface into a quadrupole mass spectrometer and, after mass analysis, they were introduced through an aspirator-like interface into flowing helium carrier gas at 0.35 ± 0.01 Torr and 295 ± 2 K. The atomic ions emerging from the atmospheric pressure plasma have a Maxwell–Boltzmann kinetic and internal energy distribution characteristic of the plasma temperature. However, these populations are downgraded by collisions with argon atoms during sampling, as well as by collisions with He in the flow tube and by radiative decay before entry into the reaction region.

Metal–glycine adduct ions were generated by adding glycine vapor directly into the flow tube from a heated stainless steel tubular inlet maintained at a fixed temperature of about 200 °C. The flow of glycine could not be adjusted for optimum adduct formation but the first adduct was predominant at the sublimation temperature employed. For example,

the ion/signal ratios Cu^+:$CuGly^+$:$Cu(Gly)_2^+$ = 66:10:1.

After experiencing about 10^5 collisions with He atoms, the ions were allowed to react with added neutral reagents. The mixture was sampled still further downstream with a second quadrupole mass spectrometer followed by an electron multiplier where reactant and product ion signals were measured as a function of added neutral reactant. The resulting profiles provide information about reaction rate coefficients, product ion distributions and reaction molecularity. Rate coefficients for the primary reactions were determined in the usual manner [31a,b] from the rate of decay of the reactant ion intensity with added neutral reagent (with an uncertainty estimated to be less than ±30%). Rate coefficients for secondary and higher-order reactions could be obtained by fitting the experimental data to solutions of differential equations for successive reactions.

The multicollision-induced dissociation (CID) [32] of sampled ions was investigated by raising the potential of the sampling nose cone from −4 to −80 V. Thresholds for dissociation are obtained from plots of relative ion intensities as a function of accelerating voltage and these provide information on bond connectivities and relative binding energies. They do not provide absolute thermochemical information since the dissociation proceeds under multicollision conditions.

The glycine sample used in this work was purchased from Sigma-Aldrich and was of 99.9% purity. Reactant neutrals were introduced into the reaction region either as mixtures in helium or as vapors diluted in helium to various levels. All neutrals were obtained commercially and were of high purity (>99.5%); the neutral reagents were used without further purification, except for D_2O that was subjected to multiple freeze–pump–thaw cycles to remove non-condensable gases. D_2O was used instead of H_2O to improve mass resolution and because of background H_2O in the buffer gas. The ammonia experiments were also performed with ND_3 to check mass assignments, but only NH_3 kinetics are reported. No significant isotope effects were evident.

Molecular orbital calculations were performed using the hybrid density functional theory (DFT) at the B3LYP level [33–35] and Salahub DZVP basis sets [36] with the Gaussian 98 program [37].

Previous calculations in our group using the same level of theory for Ag^+ bonded to oxygen and nitrogen-containing ligands [38] including amino acids [38e] have shown that computed values for binding energies are within 3.5 kcal mol^{-1} of values derived from experimental threshold measurements and the kinetic method.

3. Results of ICP-SIFT/CID kinetic experiments

Experimental results obtained for reactions of Cu^+, Ag^+, $CuGly^+$ and $AgGly^+$ with CO are presented in Fig. 1 and those for reactions of Cu^+, Ag^+, $CuGly^+$ and $AgGly^+$ with NH_3 are presented in Fig. 2. It is seen that adduct formation is the only observed reaction channel and, under the experimental conditions adopted here, it is expected to proceed by termolecular association with helium acting as a stabilizing third body. Sequential addition was observed in a number of cases. Apparent bimolecular rate coefficients for the addition reactions of glycine adducts of Cu^+ and Ag^+ with CO, D_2O and NH_3 are presented in Table 1 and those for the addition reactions of the bare Cu^+ and Ag^+ ions with the same neutrals are given in Table 2. The results for the sequential reactions of Ag^+ with ammonia agree with our previous measurements [38d].

Often deviations from linearity of the semi-logarithmic decays were observed and this indicates that the addition reactions may be reversible and approach equilibrium. The approach to equilibrium can be monitored in a plot of the product-to-reactant ion–signal ratio against the flow of reactant. Attainment of equilibrium is manifested in such a plot by the attainment of linearity since the equilibrium constant $K_{eq} = [ML^+]/([M^+][L])$. An evaluation of K_{eq} provides a measure of the standard free energy for the ligation reaction, ΔG°, since $\Delta G^\circ = -RT \ln K_{eq}$. Only a lower limit to K_{eq} (and thus an upper limit to ΔG°) can be

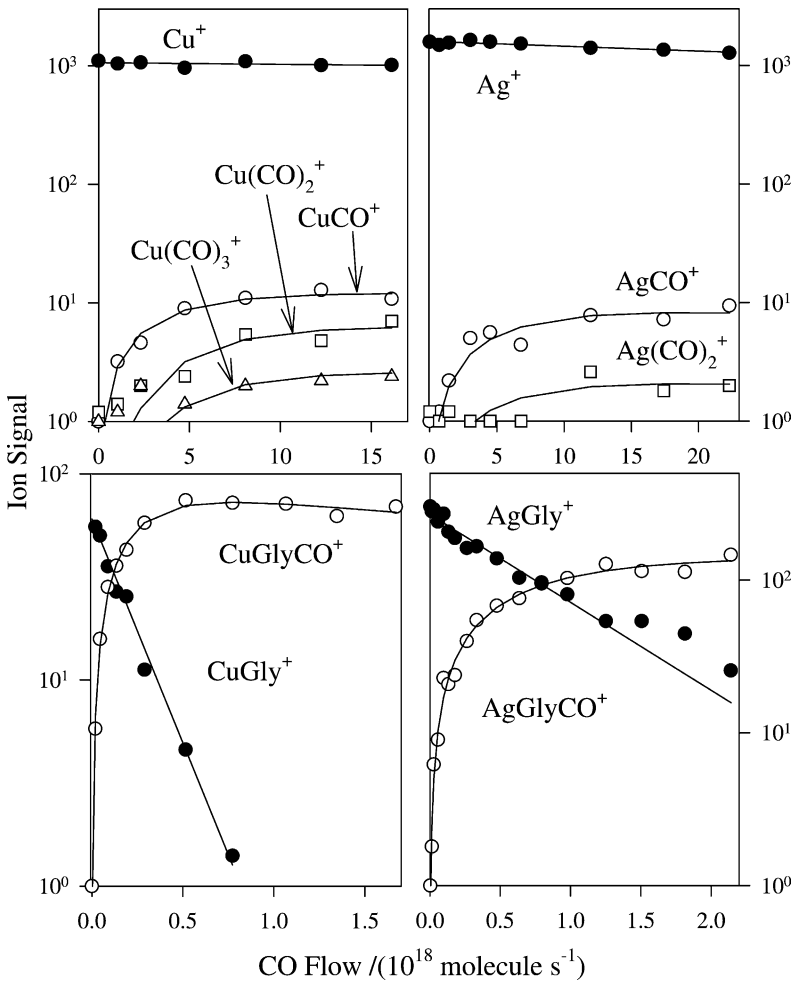

Fig. 1. Composite of experimental results for reactions of Cu^+, Ag^+, $CuGly^+$ and $AgGly^+$ with CO in helium buffer gas at 0.35 ± 0.01 Torr and 295 ± 2 K.

Table 1
Observed product ions, measured rate coefficients k, in $cm^3\,molecule^{-1}\,s^{-1}$, and collision rate coefficients k_c, in $cm^3\,molecule^{-1}\,s^{-1}$, calculated using the algorithm of the combined variational transition state theory developed by Su and Chesnavich [39] for the reactions of Cu^+–glycine and Ag^+–glycine with CO, D_2O and NH_3 at 295 ± 2 K and 0.35 ± 0.01 Torr

	$CuGly^+$			$AgGly^+$		
	Product ions	k	k_c	Product ions	k	k_c
CO	$CuGlyCO^+$	2.3×10^{-10}	7.0×10^{-10}	$AgGlyCO^+$	7.1×10^{-11}	6.9×10^{-10}
D_2O	$CuGlyD_2O^+$	5.9×10^{-10}	2.1×10^{-9}	$AgGlyD_2O^+$	3.4×10^{-10}	2.1×10^{-9}
NH_3	$CuGlyNH_3^+$	1.7×10^{-9}	2.2×10^{-9}	$AgGlyNH_3^+$	1.5×10^{-9}	2.2×10^{-9}
	$CuGly(NH_3)_2^+$	4.1×10^{-11}	1.9×10^{-9}	$AgGly(NH_3)_2^+$	3.4×10^{-11}	1.8×10^{-9}

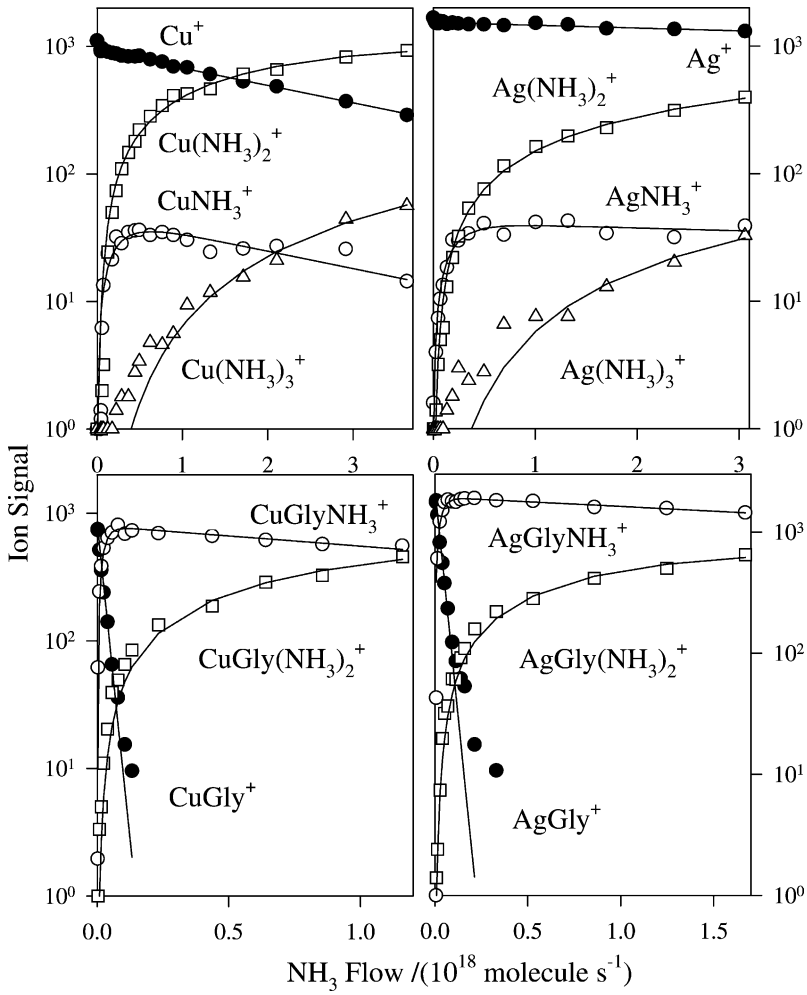

Fig. 2. Composite of experimental results for reactions of Cu^+, Ag^+, $CuGly^+$ and $AgGly^+$ with NH_3 in helium buffer gas at 0.35 ± 0.01 Torr and 295 ± 2 K.

obtained when equilibrium is not achieved. This was the case for all the addition reactions investigated in this study; Table 3 provides the limiting values for K_{eq} and ΔG° that were obtained.

3.1. Reactions of $CuGly^+$ and $AgGly^+$

The glycine mono-adducts of both Cu^+ and Ag^+ each attached one molecule of CO in relatively fast reactions, $k = 2.3 \times 10^{-10}$ cm^3 molecule^{-1} s^{-1} and 7.1×10^{-11} cm^3 molecule^{-1} s^{-1}, respectively (see Table 1). $CuGly^+$ and $AgGly^+$ added also one molecule of water with higher rate coefficients, 5.9×10^{-10} cm^3 molecule^{-1} s^{-1} and 3.4×10^{-10} cm^3 molecule^{-1} s^{-1}, respectively.

The reaction of $CuGly^+$ and $AgGly^+$ with ammonia resulted in sequential addition of two molecules. The measured (apparent bimolecular) rate coefficients for the addition of the first molecule of ammonia were 1.7×10^{-9} cm^3 molecule^{-1} s^{-1} and 1.5×10^{-9} cm^3 molecule^{-1} s^{-1}, respectively. Addition of the second molecule of ammonia to the glycine adducts of both metal cations was slower than the addition of the first molecule,

Table 2
Observed product ions, measured rate coefficients k, in $cm^3\,molecule^{-1}\,s^{-1}$ and collision rate coefficients k_c, in $cm^3\,molecule^{-1}\,s^{-1}$, calculated using the algorithm of the combined variational transition state theory developed by Su and Chesnavich [39] for reactions of Cu^+ and Ag^+ with CO, D_2O and NH_3 at 295 ± 2 K and 0.35 ± 0.01 Torr

	Cu^+			Ag^+		
	Product ions	k	k_c	Product ions	k	k_c
CO	$CuCO^+$	1.7×10^{-13}	7.7×10^{-10}	$AgCO^+$	5.4×10^{-13}	7.9×10^{-10}
	$Cu(CO)_2^+$	1.3×10^{-11}		$Ag(CO)_2^+$	9.1×10^{-12}	
	$Cu(CO)_3^+$	2.7×10^{-11}				
D_2O	CuD_2O^+	4.0×10^{-11}	2.3×10^{-9}	AgD_2O^+	6.8×10^{-12}	2.1×10^{-9}
	$Cu(D_2O)_2^+$	6.9×10^{-10}		$Ag(D_2O)_2^+$	3.4×10^{-10}	
	$Cu(D_2O)_3^+$	Observed		$Ag(D_2O)_3^+$	Observed	
	$Cu(D_2O)_4^+$	Observed				
	$Cu(D_2O)_5^+$	Observed				
NH_3	$CuNH_3^+$	1.7×10^{-11}	2.2×10^{-9}	$AgNH_3^+$	2.7×10^{-12}	2.2×10^{-10}
	$Cu(NH_3)_2^+$	1.0×10^{-9}		$Ag(NH_3)_2^+$	2.8×10^{-10}	
	$Cu(NH_3)_3^+$	2.8×10^{-12}		$Ag(NH_3)_3^+$	7.8×10^{-12}	

$k = 4.1 \times 10^{-11}\,cm^3\,molecule^{-1}\,s^{-1}$ and $3.4 \times 10^{-11}\,cm^3\,molecule^{-1}\,s^{-1}$, respectively.

3.2. Reactions of Cu^+ and Ag^+

The reactions of Cu^+ and Ag^+ with CO resulted in addition of three molecules of CO to Cu^+ and of two molecules of CO to Ag^+. The primary reaction steps were measured to have rate coefficients of $1.7 \times 10^{-13}\,cm^3\,molecule^{-1}\,s^{-1}$ and $5.4 \times 10^{-13}\,cm^3\,molecule^{-1}\,s^{-1}$, respectively, three and two orders of magnitude, respectively, slower than the reactions of the corresponding glycine mono-adducts (see Table 2).

Reactions of Cu^+ and Ag^+ with water resulted in addition of up to five molecules to Cu^+ and three molecules to Ag^+. Again, the primary reactions are slower than the reactions of the corresponding glycine adducts, $k = 4.0 \times 10^{-11}\,cm^3\,molecule^{-1}\,s^{-1}$ and $6.8 \times 10^{-12}\,cm^3\,molecule^{-1}\,s^{-1}$, respectively.

The reaction with ammonia resulted in addition of three molecules to both bare metal cations with $k = 1.7 \times 10^{-11}\,cm^3\,molecule^{-1}\,s^{-1}$ and $2.7 \times 10^{-12}\,cm^3\,molecule^{-1}\,s^{-1}$, respectively, for the primary reaction step.

Measured rate coefficients for higher-order addition of CO, D_2O and NH_3 to Cu^+ and Ag^+ are also shown in Table 2. However, rate coefficients for formation of $Cu(D_2O)_3^+$, $Cu(D_2O)_4^+$, $Cu(D_2O)_5^+$ and $Ag(D_2O)_3^+$ could not be determined in the kinetic experiments because of the low vapor pressure of water. These high-order adducts were observed by adding pure D_2O into the flow tube.

Table 3
Reaction efficiencies, $\Phi_{exp} = k/k_c$, where k is the measured rate coefficient and k_c is the collision rate coefficient calculated using the algorithm of the combined variational transition state theory developed by Su and Chesnavich [39], measured equilibrium constants for a standard state of 1 atm, K_{eq}, and free energy changes, ΔG°_{exp} (kcal mol^{-1}), for addition of CO, D_2O and NH_3 to glycine mono-adducts of Cu^+ and Ag^+

	$CuGly^+$			$AgGly^+$		
	$\Phi_{exp} = k/k_c$	K_{eq}	ΔG°_{exp} (kcal mol^{-1})	$\Phi_{exp} = k/k_c$	K_{eq}	ΔG°_{exp} (kcal mol^{-1})
CO	0.32	$>2.1 \times 10^8$	<-11.3	0.10	$>2.0 \times 10^7$	<-10.0
D_2O	0.28	$>2.7 \times 10^8$	<-11.5	0.16	$>8.8 \times 10^7$	<-10.8
NH_3	0.77	$>4.9 \times 10^8$	<-11.9	0.68	$>4.4 \times 10^8$	<11.8
	0.02	$>3.5 \times 10^6$	<-8.9	0.02	$>8.8 \times 10^5$	<-8.1

For both bare metal cations, addition of the second molecule of CO, water and ammonia was faster than the addition of the first one. In contrast, addition of the second molecule of ammonia to the glycine adducts of both metal cations was slower than the addition of the first molecule. For Cu^+ the third reaction step for addition of CO was slightly faster than the addition of the second molecule. Addition of NH_3 to $Cu(NH_3)_2^+$ was found to be considerably slower than the first two additions.

4. Discussion of experimental results

The formal site of the charge in $CuGly^+$ and $AgGly^+$ is most likely the metal centre since the ionization energies of both Cu^+ (IE = 7.73 eV) and Ag^+ (IE = 7.58 eV) are lower than that of glycine (IE = 8.9 eV) [40] so that electron transfer is not likely to occur within $CuGly^+$ and $AgGly^+$. Therefore, the site of addition of CO, water and ammonia to these complexes is likely to be the metal centre and not the glycine ligand.

The measured rate coefficients for primary reactions of both glycine adducts with the three neutral reagents increase in the order CO < D_2O < NH_3 suggesting the same order for the bond dissociation energies of both $CuGly^+$ and $AgGly^+$. The correlation between the rate coefficient of termolecular addition and the bond dissociation energy within the ligated complex has been discussed previously [41]. Electrostatic considerations indicate the same ordering CO < D_2O < NH_3 in the bond strengths since CO has a low dipole moment, $\mu(CO) = 0.112$ Debye, while ammonia and water have high dipole moments, $\mu(NH_3) = 1.47$ Debye and $\mu(D_2O) = 1.85$ Debye [42]. Although ammonia has a lower dipole moment than water, it forms stronger electrostatic bonds because the effective position of its dipole moment is closer to the metal center than the effective position of the water dipole moment [43]. The reaction efficiencies (the ratio of the measured rate coefficient to the calculated collision rate coefficient) shown in Table 3 for both $CuGly^+$ and $AgGly^+$ have similar values with CO and D_2O, much lower than the efficiencies with NH_3. This could be an indication that CO and D_2O have similar binding energies to the glycine adducts. A dative contribution to the bonding may enhance the bonding with CO vs. the bonding expected from purely electrostatic considerations.

The values of free energy change derived from our kinetic experiments are only limits as none of the systems were observed to achieve equilibrium (see Table 3). The relative ordering determined from the upper limits of the change in free energy upon ligation to both $CuGly^+$ and $AgGly^+$ is $NH_3 > D_2O > CO$.

The second addition of NH_3 to both $CuGly^+$ and $AgGly^+$ occurred with a lower rate coefficient than the first addition (see Table 1), indicating formation of a weaker bond, possibly with the second NH_3 molecule not directly coordinated to the metal centre, but forming hydrogen bonds. The upper limits determined for the change in free energy upon addition of a second molecule of NH_3 to $CuGlyNH_3^+$ and $AgGlyNH_3^+$ are lower than the limits determined for the addition of the first ammonia molecule (see Table 3). A second adduct with CO or D_2O was not observed for both $CuGly^+$ and $AgGly^+$, possibly because of their weak ligation; these adducts could have been dissociated in the sampling system due to the application of a small voltage on the nose cone [44].

All the reactions of bare metal cations are slow, presumably because of the reduced number of degrees of freedom available for energy redisposition within the intermediate ML^+ complex against dissociation into reactants. Known binding energies of CO, H_2O and NH_3 to Cu^+ and Ag^+ determined experimentally and computationally are presented in Table 4.

The faster addition of a second molecule of ligand to both Cu^+ and Ag^+ observed in our experiments reflects the increase of number of degrees of freedom upon addition of one molecule to the metal cation, as discussed previously for the addition of ammonia to Ag^+ [38]. However, the faster addition of the second ligand could also be a reflection of the higher binding energy for the second ligand, as determined experimentally and calculated by several research groups for reactions of a variety of late transition metal

Table 4
Experimental and calculated bond dissociation energies

	Cu^+		Ag^+	
	Experimental	Calculated	Experimental	Calculated
M^+–CO	35.5 ± 1.6[a]	32.3[b]	21.3 ± 1.2[a]	21.8[b]
$(CO)M^+$–CO	41.1 ± 0.7[a]	36.2[b]	26.1 ± 1.0[a]	26.4[b]
$(CO)_2M^+$–CO	17.9 ± 0.9[a]	18.6[b]	13.1 ± 1.9[a]	12.6[b]
$(CO)_3M^+$–CO	12.7 ± 0.7[a]	16.5[b]	12.9 ± 2.4[a]	11.1[b]
M^+–H_2O	35 ± 3[c]	35.9[d]	33.3 ± 2.2[c]	31.9[f]
$(H_2O)M^+$–H_2O	39 ± 3[c]	37.3[d]	25.4 ± 0.3[c]	28.0[f]
$(H_2O)_2M^+$–H_2O	17 ± 2[c]	15.1[d]	15.0 ± 0.1[c]	12.4[f]
$(H_2O)_3M^+$–H_2O	15 ± 3[c]	13.8[d]	14.9 ± 0.2[e]	13.4[f]
M^+–NH_3	56 ± 3.6[h]	50.8[d]	∼48.7[g]	46.2[f]
$(NH_3)M^+$–NH_3	59 ± 2.4[h]	52.8[d]	36.9 ± 0.8[e]	36.1[i]
$(NH_3)_2M^+$–NH_3	11 ± 1.4[h]	15.6	14.6 ± 0.1[e]	15.1[i]
$(NH_3)_3M^+$–NH_3	11 ± 1.4[h]	14.0[d]	13.0 ± 0.1[e]	11.0[i]

[a] Values of D_0 from [45].
[b] D_{298} from [46].
[c] 298 K values for DE from [47].
[d] ZPE corrected values from [48].
[e] 298 K values for the reaction enthalpy from [49].
[f] 298 K values for binding enthalpy from [50].
[g] ΔH^0 values from [51].
[h] 298 K values for binding enthalpies from [52].
[i] 298 K values for binding enthalpies from [38].

cations including Cu^+ and Ag^+ with NH_3, H_2O, CO (see Table 4) [38,45–52]. The higher binding energy for the second molecule of ligand has been explained by the ability of transition metal cations to use s–d σ-hybridization to reduce the repulsion with the first incoming ligand; as a result, electron density is also being placed in a direction perpendicular to the bonding axis. The second ligand can therefore "see" a higher nuclear charge when approaching from the side opposite to the first ligand and bind even stronger than the first ligand since the first ligand had to pay the energetic cost for hybridization [48]. The bonding of a third ligand to both Cu^+ and Ag^+ is weaker than the bonding of both first and second molecules due to the attenuation of s–d σ-hybridization and to increasing metal–ligand and ligand–ligand repulsion [48]. Direct coordination of all three ligand molecules to the metal center is the preferred structure of the $M(L)_3^+$ adduct, with L = CO, H_2O and NH_3 [38,46,48]. Our experiments indicate a slightly higher rate for the addition of the third CO ligand to Cu^+, but this is probably a result of an increased lifetime due to an increased number of degrees of freedom.

All the reactions of metal–glycine cations are faster than the reactions of the bare metal cations by up to three orders of magnitude. We can expect an increase because of an increase in the lifetime of the intermediate ligated metal–glycine cation due to an increase in the number of degrees of freedom available for energy redisposition within the intermediate, and so an increase in the probability of collisional stabilization. In a comparison of reaction rates of the ligation of the metal–glycine cations to those of the second ligation of the bare metal cations, it is interesting to note that CO, D_2O and NH_3 are similarly effective as glycine in increasing the lifetime, viz. as "heat sinks". There is an exact match in the rate coefficient, $k = 3.4 \times 10^{-10}\,cm^3\,molecule^{-1}\,s^{-1}$, for the reactions of $Ag(D_2O)^+$ and $AgGly^+$ with D_2O. The corresponding values for $Cu(D_2O)^+$ and $CuGly^+$ are $6.9 \times 10^{-10}\,cm^3\,molecule^{-1}\,s^{-1}$ and

5.9×10^{-10} cm^3 molecule^{-1} s^{-1}, respectively. For CO and NH_3 the rate coefficients for the metal–glycine cation reactions are about 2–20 times larger than those for the reactions of $M(L)^+$ and this also is the case for the reactions of $MGly(L)^+$ and $M(L)_2{}^+$. So for these systems the glycine leads to a higher increase in the intermediate lifetime than the ligand and so appears to act as a better heat sink. These comparisons are instructive but only qualitative as they do not take into account the influence of the depth of the potential well on the lifetime of the intermediate [41].

A comparison of reactivities of the silver and copper glycine mono-adducts to the same neutral reagent indicates slight differences. For the reactions with CO and D_2O, $CuGly^+$ gives larger rate coefficients (and reaction efficiencies) than $AgGly^+$, while in the reactions with NH_3 similar values for the rate coefficients (and reaction efficiencies) are obtained (see Table 1). This could be an indication that ligation to $CuGly^+$ leads to formation of stronger bonds than ligation to $AgGly^+$. CIDs of $CuGlyCO^+$ and $AgGlyCO^+$ evident in the data shown in Fig. 3 indicate that, indeed, dissociation of $AgGlyCO^+$ to produce $AgGly^+$ proceeds at a lower laboratory-frame energy than dissociation of $CuGlyCO^+$ into $CuGly^+$ and CO, viz. 15 V vs. 25 V. Although quantitative information about bond dissociation energies cannot be derived from these onsets because of multicollision conditions, the substantial difference in the onsets of 10 V is consistent with $D(CuGly^+–CO) > D(AgGly^+–CO)$. Certainly this would be the case were these onsets to apply to single-collision conditions, especially since the mass difference between $CuGlyCO^+$ and $AgGlyCO^+$ would lead to a higher conversion of laboratory energy to centre-of-mass energy for the lower-mass $CuGlyCO^+$ ion. The equilibrium analysis performed in this study (see Table 3) also indicates more negative values (although only limiting values) of the change in free energy for all the ligation reactions of $CuGly^+$ compared with the ligation reactions of $AgGly^+$.

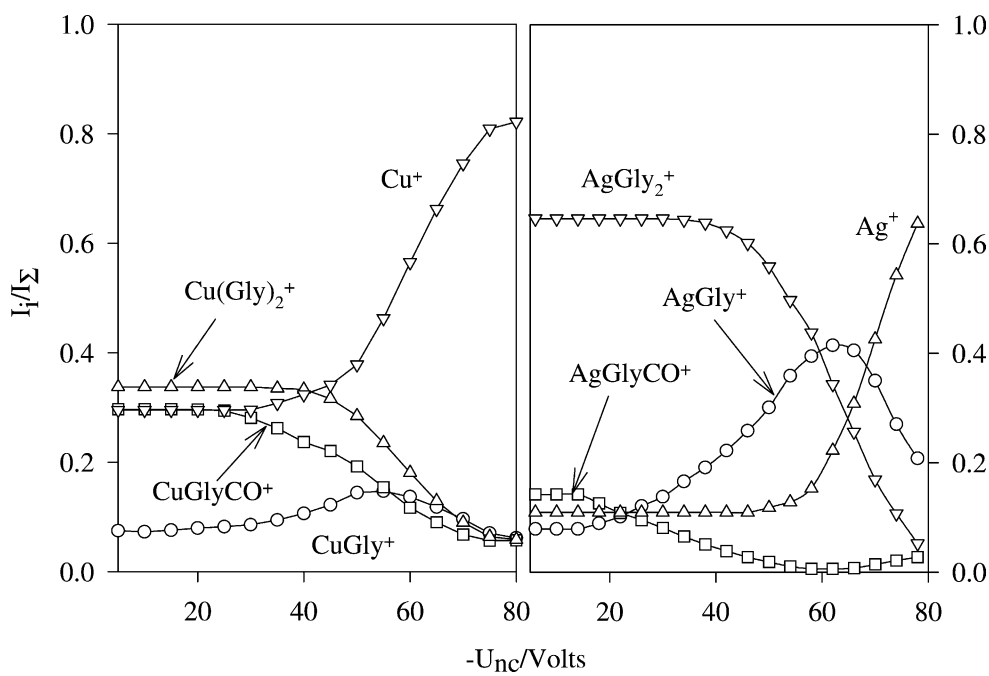

Fig. 3. Multicollision-induced dissociation spectra for $CuGlyCO^+$ and $AgGlyCO^+$ in He buffer gas at 0.35 ± 0.01 Torr.

The stronger bonding of CO, H_2O and NH_3 to $CuGly^+$ than to $AgGly^+$ seems to be a result of Cu^+ forming stronger bonds than Ag^+. Sequential binding of these molecules to Cu^+ leads to higher bond dissociation energies than the binding to Ag^+, as shown in Table 4. There are two reasons for the stronger bonds observed with Cu^+. First, the ionic radius of Cu^+ is smaller than that of Ag^+ and therefore the metal–ligand bond distances are shorter in Cu^+–L than in Ag^+–L. From an electrostatic point of view, this results in stronger bonds with Cu^+. Second, the energy difference between the ground state and the first excited state of Cu^+ is 3.26 eV compared with 5.71 eV for Ag^+ [45]. As a result, s–d σ-hybridization is more easily attained for Cu^+ and the enhancement in bond energy is larger. Although in our experiments Cu^+ is already bonded to glycine, its stronger binding capability is preserved.

4.1. Results and discussion of B3LYP/DZVP theoretical calculations

Although the sequential binding of CO, H_2O and NH_3 to the bare Cu^+ and Ag^+ ions and the structures of the resulting complexes have been studied extensively in the past 20 years, this has not been the case for Cu^+ and Ag^+ already coordinated to glycine, to the best of our knowledge. Therefore, theoretical

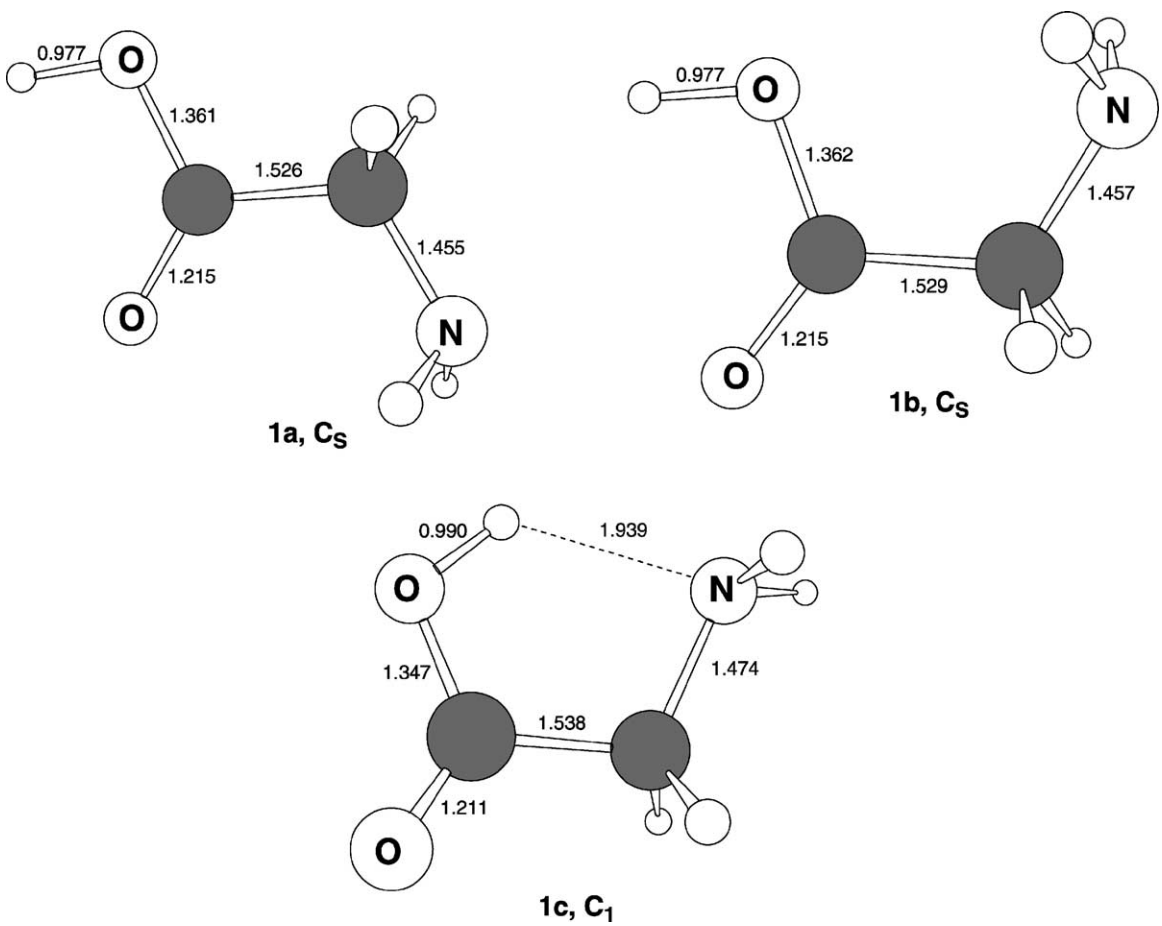

Fig. 4. Computed structures of glycine optimized at B3LYP/DZVP. Bond lengths are in Angstroms and angles are in degrees.

calculations were performed to investigate binding energies and possible structures of the adduct ions observed experimentally in this study.

4.2. Optimized structures and free energy changes for ligation

The structure of neutral glycine in the gas phase has been the subject of several extensive investigations [26a–d,28a–d]. The structures of the three lowest energy conformers that we have previously computed are shown in Fig. 4 [25]. The structures of $CuGly^+$ and $AgGly^+$ have been optimized using the lowest energy conformer of neutral glycine, **1a** in Fig. 4, which is most likely to be the structure of glycine present in our gas-phase experiments. The lowest energy structures of $CuGly^+$, **2a**, and $AgGly^+$, **3a**, presented in Fig. 5 have the metal cation di-coordinated to glycine through the amino nitrogen and the carbonyl oxygen, as reported previously [22–25]. Free energy changes of -61.8 and $-40.7\,kcal\,mol^{-1}$, respectively, were calculated for addition of glycine to Cu^+ and Ag^+. The values for the free energy change for the formation of the most stable adduct species are listed in Table 5.

The adducts produced from addition of a molecule of CO to $CuGly^+$ and $AgGly^+$ were calculated to have structures **4a** and **5a**, respectively (see Fig. 5), with the corresponding free energy changes of -27.8

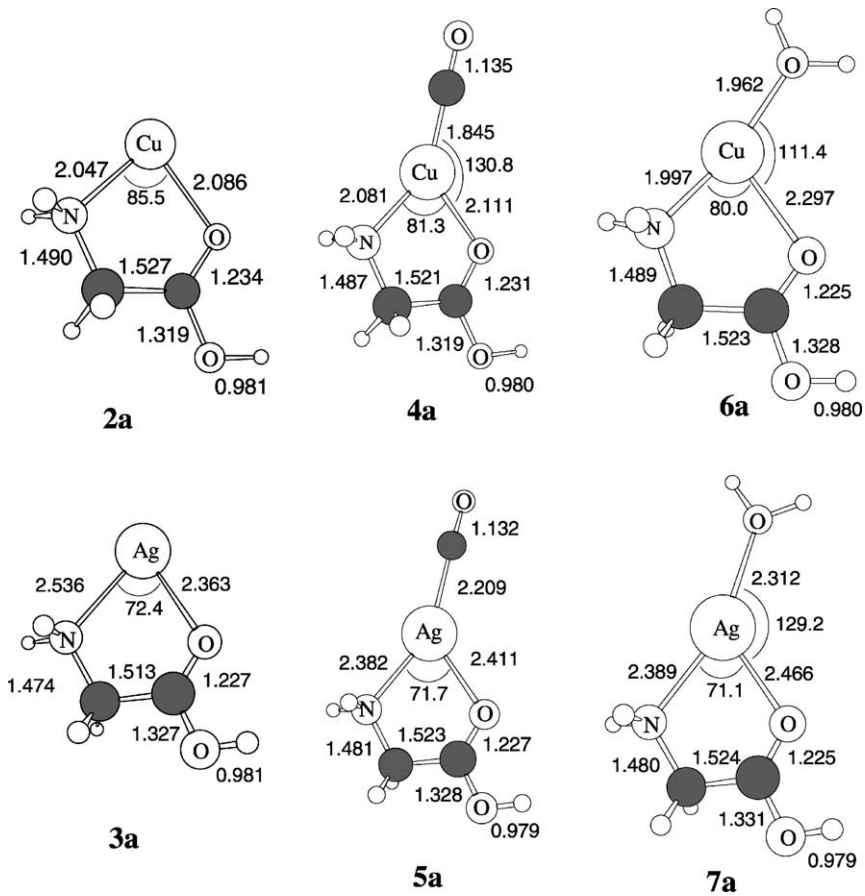

Fig. 5. Computed structures of global minima copper and silver-containing complexes. All structures are optimized at B3LYP/DZVP. Bond lengths are in Angstroms and angles are in degrees.

Table 5
Calculated free energy change ΔG°_{calc} (in kcal mol^{-1}) for addition of CO, H_2O and NH_3 to mono-adducts of glycine with Cu^+ and Ag^+

	$CuGly^+$		$AgGly^+$	
	$\Phi_{exp} = k/k_c$	ΔG°_{calc} (kcal mol^{-1})	$\Phi_{exp} = k/k_c$	ΔG°_{calc} (kcal mol^{-1})
CO	0.32	−27.8	0.10	−9.3
H_2O	0.28	−24.6	0.16	−14.5
NH_3	0.77	−37.6	0.68	−23.7
	0.02	−11.6	0.02	−8.9

and −9.3 kcal mol^{-1}, as shown in Table 5. Both structures have the CO molecule directly attached to the metal centre through the carbon, but ligation of CO to $CuGly^+$ is stronger than ligation to $AgGly^+$, in agreement with results of our multi-CID experiments shown in Fig. 3.

Coordination of H_2O to $CuGly^+$ resulted in structure **6a** while coordination of H_2O to $AgGly^+$ resulted

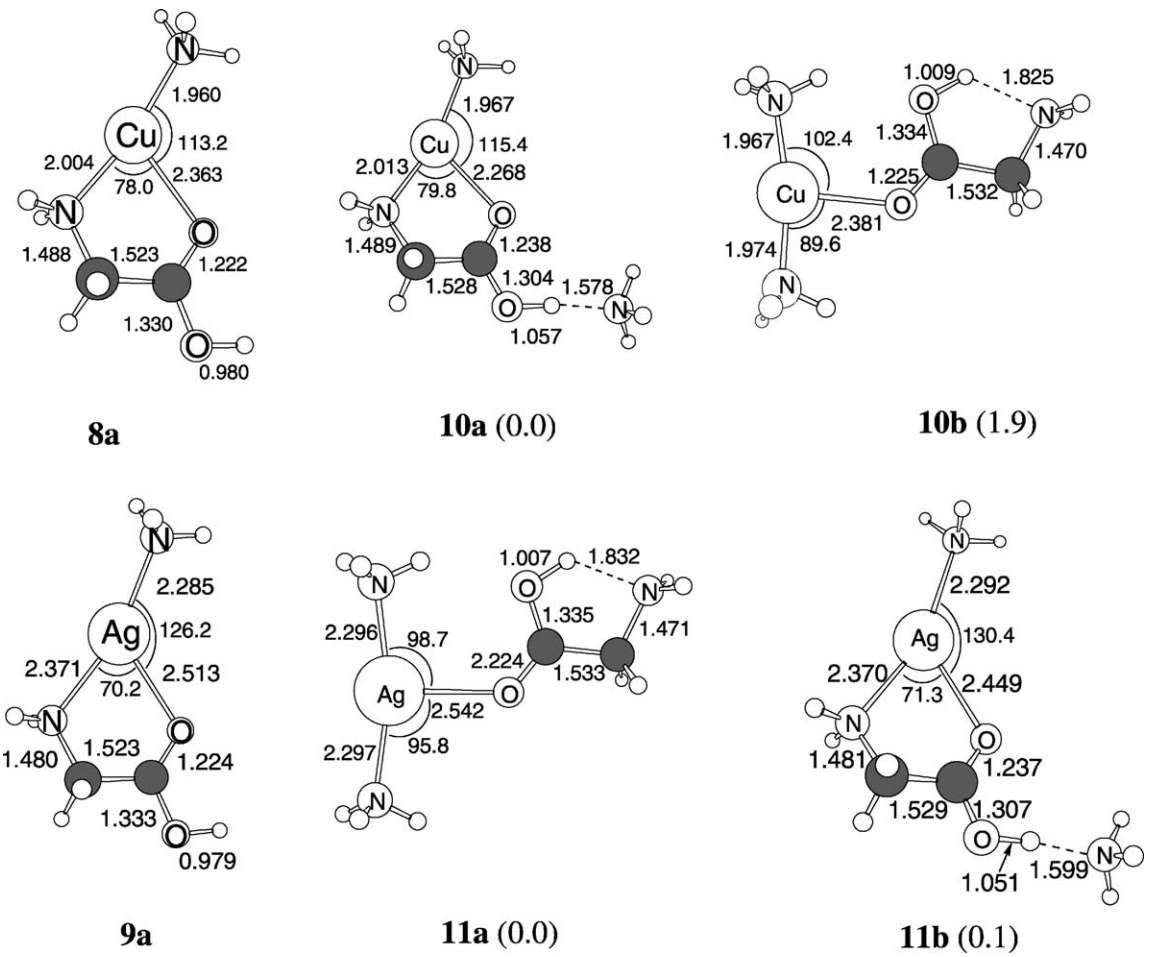

Fig. 6. Computed structures of ammonia–copper–glycine and ammonia–silver–glycine complexes. All structures are optimized at B3LYP/DZVP. Bond lengths are in Angstroms and angles are in degrees.

in structure **7a**; both structures again have the metal centre tri-coordinated, with the glycine amino nitrogen and carbonyl oxygen and with the water ligand, as shown in Fig. 5. Free energy changes of −24.6 and −14.5 kcal mol^{-1}, respectively were calculated for these ligation reactions (Table 5).

Ligation of one NH_3 molecule to structures $CuGly^+$ and $AgGly^+$ produced structures **8a** and **9a**, with NH_3 directly coordinated to the metal centre (Fig. 6). The corresponding free energy changes for these reactions were calculated to be −37.6 and −23.7 kcal mol^{-1}, respectively (see Table 5). Again, coordination to $CuGly^+$ results in stronger bonds than coordination to $AgGly^+$, and in both cases the calculated changes in free energies exceed ΔG° for addition of either CO or water.

Coordination of a second molecule of NH_3 to both $CuGlyNH_3^+$ and $AgGlyNH_3^+$ was also investigated computationally. For $CuGly(NH_3)_2^+$ the lowest energy structure is structure **10a** in which the first molecule of ammonia coordinated at the metal centre and the second molecule of ammonia is involved in hydrogen bonding with the hydrogen of the carboxy group (see Fig. 6). The glycine remains attached through both the amino N and the carbonyl O. Structure **10b** is 1.9 kcal mol^{-1} higher in energy; both ammonia molecules are coordinated to the metal centre and the glycine is only coordinated through the carbonyl O atom. A third structure (not shown) involving direct coordination of both ammonia molecules and the amino group of glycine lies 5.7 kcal higher in free energy. The change in free energy for addition of NH_3 to $CuGlyNH_3^+$ leading to structure **10a** is −11.6 kcal mol^{-1}, much lower than the change in free energy for addition of NH_3 molecule to $CuGly^+$ (see Table 5).

For $AgGly(NH_3)_2^+$, structure **11a**, where Ag^+ is directly coordinated by two molecules of ammonia and by glycine attached through only the carbonyl O atom (analogous to the copper structure **10b**) is 0.1 kcal mol^{-1} lower in energy than structure **11b** (analogous to the copper structure **10a**). The structure involving direct coordination of the two ammonia molecules and the amino group of glycine is only 0.9 kcal mol^{-1} higher than structure **11a**. In this case, in contrast to the Cu structure, there is an additional interaction between the carbonyl oxygen and silver ion and this may account for the additional stabilization. The free energy change for addition of NH_3 to $AgGlyNH_3^+$, structure **9a**, to generate $AgGly(NH_3)_2^+$, structure **11a**, is −8.9 kcal mol^{-1} (Table 5). In the formation of complexes with both $CuGly^+$ and $AgGly^+$, the second molecules of ammonia form weaker bonds than the first ones, in agreement with our kinetic data (Tables 1 and 3).

Table 5 summarizes the experimental results and the calculations for reactions of $CuGly^+$ and $AgGly^+$ with the three ligands. A good correlation is found between the experiment and the calculations. Fig. 7 displays nearly linear dependencies of the experimentally determined reaction efficiencies and the calculated free energy changes. The first ligation with NH_3 appears to produce a slight upward curvature presumably due to a slightly higher intermediate lifetime because of the slightly higher number of degrees of freedom of NH_3 compared to CO and D_2O.

4.3. Interconversion from the charge solvated to metal salt form of the adducts

Although the zwitterionic form of glycine is not at a minimum on the potential energy surface, in the presence of a metal cation the zwitterionic form of the complex metal cation–glycine, the so-called “metal salt”, is at a minimum [29a–d]. We investigated computationally the effect of the metal cation alone and of the metal cation attached to a ligand (CO or NH_3) on the differences in stability of the neutral forms vs. the zwitterionic forms of the glycine complexes. The interconversions from the neutral forms to the zwitterionic forms of the glycine complexes were investigated by calculating the structures and transition states for the transition from the “charge solvated” form of the adducts (discussed previously) and the “metal salt” form of the same complexes that involve coordination with the zwitterionic form of glycine.

Computed structures for the unligated and ligated “salt” forms are shown in Fig. 8. In the unligated

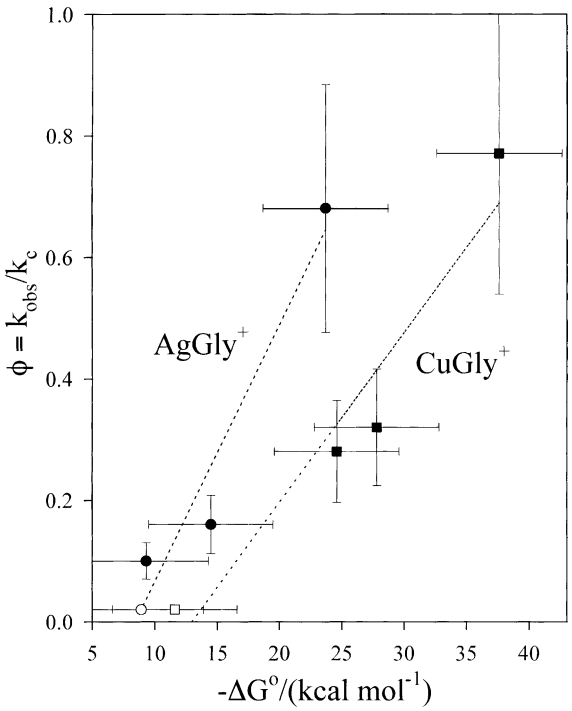

Fig. 7. Correlation of experimental reaction efficiencies ($\Phi_{exp} = k/k_c$, where k is the measured rate coefficient in helium at 295±2 K and 0.35±0.01 Torr and k_c is the collision rate coefficient calculated using calculated using the algorithm of the combined variational transition state theory developed by Su and Chesnavich [39]) and B3LYP/DZVP calculated free energy changes for ligation of CO, D_2O and NH_3 to $CuGly^+$ and $AgGly^+$ (see Table 5). The open symbols refer to the second addition of NH_3. The uncertainties in the calculation are taken to be ±5 kcal mol^{-1}.

structure **12(2g)** the copper ion is attached to only one oxygen of the carboxylate group and the other oxygen is hydrogen-bonded to the terminal NH_3^+ group. Ligation with CO, structure **13**, and NH_3, structure **14**, results in the shortening of the hydrogen bond and more so with the stronger electron-donating NH_3 ligand. In contrast to the analogous copper complex, the unligated silver adduct **15** has the metal attached to both oxygen atoms of the carboxyl group. Again there is a hydrogen bond between one of the oxygen atoms of the carboxylate group and the NH_3^+ group. It is slightly longer because of the additional Ag–O interaction. Adding the CO ligand sharply reduces the length of the hydrogen bond and the even stronger NH_3 ligand and can result in the migration of a proton from NH_3^+ to the carboxylate group.

The results of the B3LYP/DZVP calculations for the interconversion between the "charge solvated" species and the "metal salt" species for adducts of Cu^+ and Ag^+ with glycine and for adducts of $CuGly^+$ and $AgGly^+$ with CO and NH_3 are summarized in Table 6. The tabulated results provide a comparison of the free energy change for formation of the "charge solvated" and "metal salt" species. Also indicated is the barrier height for the interconversion between the two forms of adducts, defined as the difference in free energy between the most stable species on the potential energy hypersurface (the "charge solvated" adduct) and the highest energy structure (a transition state). It can be seen from Table 6 that this barrier is much more sensitive to ligation in the case of Cu. Finally, the difference in free energy between the two adduct species is included in Table 6 for a comparison of the Cu and Ag adducts. For the silver adducts this difference is ca. 4.5 kcal mol^{-1} and is insensitive to the presence of a ligand. In the case of Cu, for which the unligated salt form is 9.2 kcal mol^{-1} higher in energy than the charge solvated form, ligands reduce this difference to 6.1 for CO to 3.5 kcal mol^{-1} for NH_3. Also included in Table 6 are the free energies for all the intermediates and the two other transition states involved in all six interconversions. For three of these interconversions, those involving ammonia as a ligand and that for CO ligated to $AgGly^+$, the last step involving proton migration is endoergic. Fig. 9 shows the full free energy profile for the conversion of the unligated Cu adduct. Also shown are the structures of the intermediates and transition states on this profile. The remaining structures and free energy profiles have been reported elsewhere [53].

All interconversions follow the same mechanistic pathway. In the first step the metal–NH_2 bond is broken and the NH_2 group rotates away from the metal. The second step involves rotation about the C–OH bond to form a hydrogen bond with the amino group. This step is rate determining since the transition state which involves the disruption of conjugation in the carboxyl group lies highest in the overall

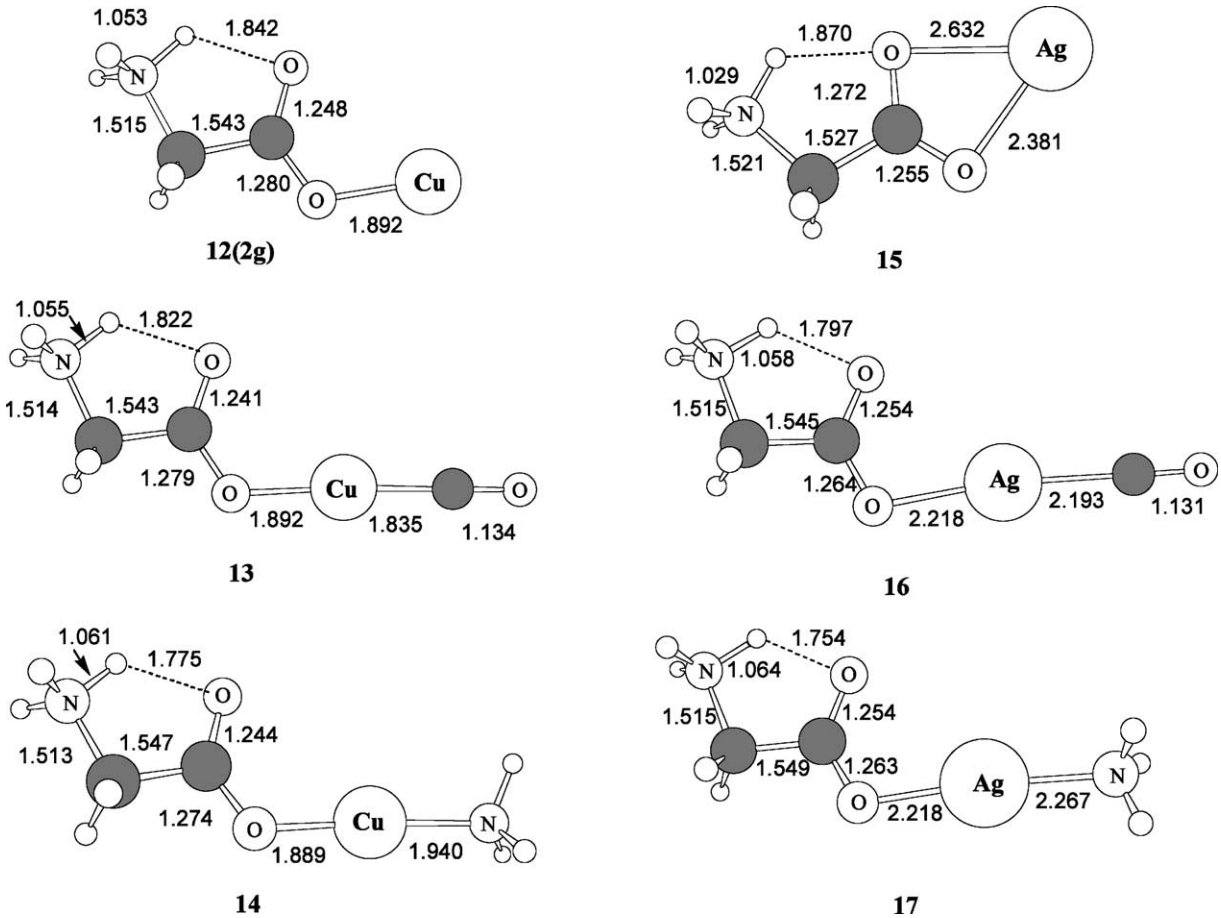

Fig. 8. Computed structures for the unligated and ligated "salt" forms of cationic copper–glycine and silver–glycine complexes. All structures are optimized at B3LYP/DZVP. Bond lengths are in Angstroms and angles are in degrees.

Table 6
Computed free energies (in kcal mol^{-1} with respect to the global minimum) for intermediates and transition states (designated with an asterisk) in the conversion of the charge solvated to the metal salt forms of glycine adduct ions

	ΔG_i° [a]	a	b*	c	d*, [b]	e	f*	g [c]
Cu^+–Gly	61.8	0	28.0	26.5	33.6	11.6	12.6	9.2
$CuGly^+$–CO	27.8	0	22.9	21.5	28.4	7.8	8.9	6.1
$CuGly^+$–NH_3	37.6	0	16.2	15.8	22.8	3.0	5.3	3.5
Ag^+–Gly	40.7	0	19.6	16.9	26.5	5.6	7.4	4.5
$AgGly^+$–CO	9.3	0	16.5	15.3	25.4	3.8	6.2	4.6
$AgGly^+$–NH_3	23.7	0	13.6	12.3	24.8	2.8	4.8	4.5

Intermediates and transition states are labeled according to the code in Fig. 9.

[a] Free energy of the separated species with respect to the global minimum.

[b] Barrier height for the interconversion defined as the free energy of the highest transition state with respect to the global minimum.

[c] Difference in free energy between the charge solvated and metal salt species.

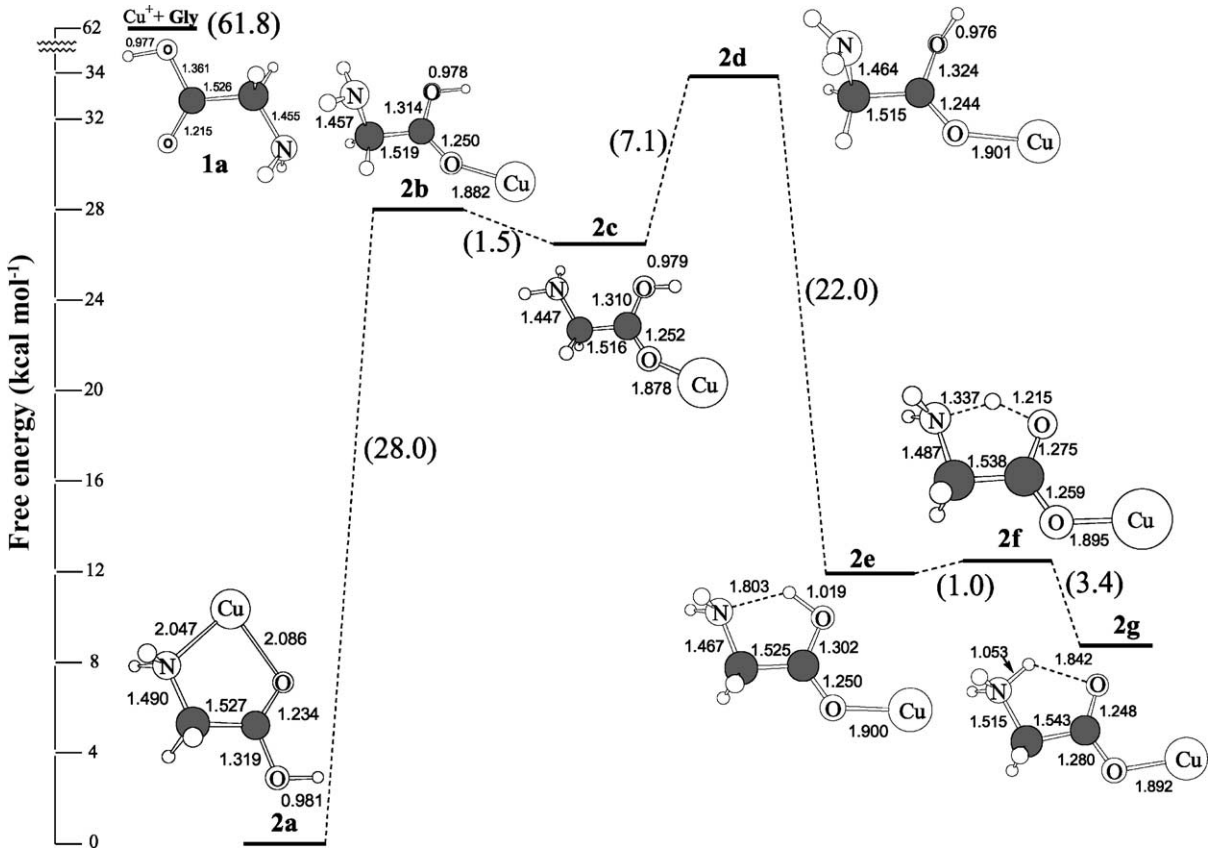

Fig. 9. Potential energy surface for the interconversion of the $CuGly^+$ complex. Structure numbers are in bold; values in parentheses are free energy differences in kcal mol^{-1} with respect to the global minimum.

profile. The last step simply involves the migration of a proton across the hydrogen bond and therefore has a low barrier but, as we have seen, is endoergic in three of the six cases.

5. Conclusions

The reactivities of the $CuGly^+$ and $AgGly^+$ complexes have been compared with the reactivities of the metal cations towards the same neutral reagents: CO, D_2O and NH_3. All observed reactions resulted in adduct formation, presumably with helium buffer gas acting as a stabilizing agent. Higher rate coefficients (by as much as three orders of magnitude) and a smaller degree of ligation characterizes the chemistry of $CuGly^+$ and $AgGly^+$ when compared with the chemistry of Cu^+ and Ag^+. Irrespective of the reagent, ligation to $CuGly^+$ is stronger than to $AgGly^+$ and, in both instances, ligation of carbon monoxide and water has comparable strengths, while much stronger coordination is achieved with ammonia.

B3LYP/DZVP theoretical calculations confirmed that $CuGly^+$ forms stronger adducts than $AgGly^+$. For all adducts the "charge solvated" form is found to be more stable than the "metal salt". A good correlation was obtained between the experimental reaction efficiencies and the calculated free energy changes upon ligation of CO, D_2O and NH_3. The potential energy surfaces for interconversion between

the "charge solvated" forms to the "metal salt" forms of the species $CuGly^+$, $AgGly^+$, and of their adducts with CO or NH_3 have also been investigated and the results are presented. A modest "catalytic" effect was identified theoretically for the influence of CO and NH_3 on the interconversion between the "charge solvated" and "metal salt" adduct ions.

Acknowledgements

Continued financial support from the Natural Sciences and Engineering Research Council of Canada is greatly appreciated. Also, we acknowledge support from the National Research Council, the Natural Science and Engineering Research Council and MDS SCIEX in the form of a Research Partnership grant. As holder of a Canada Research Chair in Physical Chemistry, Diethard K. Bohme thanks the Canada Research Chair Program for its contributions to this research. We thank the reviewers for useful input.

References

[1] P.B. Armentrout, Ann. Rev. Phys. Chem. 52 (2001) 423.
[2] B.S. Freiser (Ed.), Organometallic Ion Chemistry, Kluwer Academic Publishers, Dordrecht, 1996, and references cited therein.
[3] K. Eller, H. Schwarz, Chem. Rev. 91 (1991) 1121.
[4] J. Sauer, Chem. Rev. 89 (1989) 199.
[5] J.-E. Bäckvall, F. Bökman, M.R.A. Blomberg, J. Am. Chem. Soc. 114 (1992) 534.
[6] D.A. Dougherty, Science 271 (1966) 163.
[7] R.K. Silagyi, G. Frenking, Organometallics 16 (1997) 4807.
[8] J.P. Glusker, Adv. Protein Chem. 42 (1991) 1.
[9] S.J. Lippard, J.M. Berg, Principles of Bioinorganic Chemistry, University Science Books, Mill Valley, CA, 1994.
[10] M.N. Hughes, The Inorganic Chemistry of Biological Processes, 2nd ed., Wiley, Chichester, 1981.
[11] W. Kaim, B. Schwederski, Bioinorganic Chemistry: Inorganic Elements in the Chemistry of Life, Wiley, Chichester, 1994.
[12] K.D. Karlin, J. Zubieta, Copper Coordination Chemistry: Biological and Inorganic Perspectives, Adenine, Guilderland, NY, 1983.
[13] N. Farrell, Transition Metal Complexes as Drugs and Chemotherapeutic Agents, Kluwer Academic Publishers, Dordrecht, 1989.
[14] I.K. Chu, X. Guo, T.-C. Lau, K.W.M. Siu, Anal. Chem. 71 (1999) 2364.
[15] S.-W. Lee, H.S. Kim, J.L. Beauchamp, J. Am. Chem. Soc. 120 (1998) 3188.
[16] T. Lin, G.L. Glish, Anal. Chem. 70 (24) (1998) 5162.
[17] S. Bouchonnet, Y. Hoppilliard, G. Ohanessian, J. Mass Spectrom. 30 (1995) 172.
[18] C.L. Gatlin, F. Turecek, J. Mass Spectrom. 30 (1995) 1605.
[19] C. Seto, J.A. Stone, Int. J. Mass. Spectrom. 192 (1999) 289.
[20] B.A. Cerda, L. Cronett, C. Wesdemiotis, Int. J. Mass Spectrom. 193 (1999) 205.
[21] V.W.-M. Lee, H.T.-C. LiLau, R. Guevremont, K.W.M. Siu, J. Am. Soc. Mass Spectrom. 9 (1998) 760.
[22] S. Hoyau, G. Ohanessian, J. Am. Chem. Soc. 119 (1997) 2016.
[23] J. Bertran, L. Rodriguez-Santiago, M. Sodupe, Phys. J. Chem. B 103 (1999) 2310.
[24] T. Marino, N. Russo, M. Toscano, J. Inorg. Biochem. 79 (2000) 179.
[25] T. Shoeib, C.F. Rodriguez, K.W.M. Siu, A.C. Hopkinson, Phys. Chem. Chem. Phys. 3 (2001) 853.
[26] (a) R.D. Suenram, F.J. Lovas, J. Mol. Spectrosc. 72 (1978) 372;
(b) R.D. Brown, P.D. Godfrey, J.W.V. Storey, M.-P.J. Bassez, Chem. Soc. Chem. Commun. (1978) 547;
(c) K. Iijima, K. Tanaka, S. Onuma, J. Mol. Struct. 246 (1991) 257;
(d) F.J. Lovas, Y. Kawashima, J.-U. Grabow, R.D. Suenram, G.T. Fraser, E. Hirota, Astrophys. J. 455 (1995) L201.
[27] G. Wada, E. Tamura, M. Okina, M. Nakamura, Bull. Chem. Soc. Jpn. 55 (1982) 3064.
[28] (a) Y.-C. Tse, M.D. Newton, S. Vishveshwara, J.A. Pople, J. Am. Chem. Soc. 100 (1978) 4329;
(b) Y. Ding, K. Krogh-Jespersen, Chem. Phys. Lett. 199 (1992) 261;
(c) J.H. Jensen, M.S. Gordon, J. Am. Chem. Soc. 117 (1995) 8159;
(d) M. Nagaoka, N. Okuyama-Yoshida, T. Yamabe, J. Phys. Chem. A102 (1998) 8202.
[29] (a) S. Hoyau, G. Ohanessian, Chem. Eur. J. 4 (1998) 1561;
(b) S. Bouchonnet, Y. Hoppilliard, Org. Mass. Spectrom. 27 (1992) 71;
(c) J.P. Bouchonnet, J.P. Flament, Y. Hoppilliard, Rapid Commun. Mass Spectrom. 7 (1993) 470;
(d) F. Jensen, J. Am. Chem. Soc. 114 (1992) 9533.
[30] G.K. Koyanagi, V.V. Lavrov, V. Baranov, D. Bandura, S. Tanner, J.W. McLaren, D.K. Bohme, Int. J. Mass Spectrom. 194 (2000) L1.
[31] (a) G.I. Mackay, G.D. Vlachos, D.K. Bohme, H.I. Schiff, Int. J. Mass Spectrom. Ion Phys. 36 (1980) 259;
(b) V. Baranov, D.K. Bohme, Int. J. Mass Spectrom. Ion Process. 149/150 (1995) 543.
[32] V. Baranov, D.K. Bohme, Int. J. Mass Spectrom. Ion Process. 154 (1996) 71.
[33] (a) P. Hohenberg, W. Kohn, Phys. Rev. B 136 (1964) 864;
(b) W. Kohn, L.J. Sham, Phys. Rev. A 140 (1965) 1133.
[34] (a) A.D. Becke, J. Chem. Phys. 97 (1992) 9173;
(b) A.D. Becke, J. Chem. Phys. 96 (1992) 2155;
(c) A.D. Becke, J. Chem. Phys. 98 (1993) 5648.

[35] C. Lee, W. Yang, R.G. Parr, Phys. Rev. B 37 (1988) 785.
[36] (a) N. Godbout, D.R. Salahub, J. Andzelm, E. Wimmer, Can. J. Chem. 70 (1992) 560;
(b) N. Godbout, Ensemble de base pour la théorie de la fonctionnelle de la densité, Structures moléculaires, propriétés mono-électroniques et modèles de zéolites, Département de Chimie, Faculté des Arts et des Sciences, Université de Montréal, 1996.
[37] M.J. Frisch, G.W. Trucks, H.B. Schlegel, G.E. Scuseria, M.A. Robb, J.R. Cheeseman, V.G. Zakrzewski, J.A. Montgomery, R.E. Stratmann, J.C. Burant, S. Dapprich, J.M. Millam, A.D. Daniels, K.N. Kudin, M.C. Strain, O. Farkas, J. Tomasi, V. Barone, M. Cossi, R. Cammi, B. Mennucci, C. Pomelli, C. Adamo, S. Clifford, J. Ochterski, G.A. Petersson, P.Y. Ayala, Q. Cui, K. Morokuma, D.K. Malick, A.D. Rabuck, K. Raghavachari, J.B. Foresman, J. Cioslowski, J.V. Ortiz, B.B. Stefanov, G. Liu, A. Liashenko, P. Piskorz, I. Komaromi, R. Gomperts, R.L. Martin, D.J. Fox, T. Keith, M.A. Al-Laham, C.Y. Peng, A. Nanayakkara, C. Gonzalez, M. Challacombe, P.M.W. Gill, B.G. Johnson, W. Chen, M.W. Wong, J.L. Andres, M. Head-Gordon, E.S. Replogle, J.A. Pople, Gaussian 98 (Revision A.7), Gaussian, Inc., Pittsburgh, PA, 1998.
[38] (a) H. El Aribi, T. Shoeib, C.F. Rodriquez, A.C. Hopkinson, K.W.M. Siu, J. Phys. Chem. A 106 (2002) 2908;
(b) T. Shoeib, H. El Aribi, K.W.M. Siu, A.C. Hopkinson, J. Phys. Chem. A 105 (2001) 710;
(c) H. El Aribi, C.F. Rodriquez, T. Shoeib, Y. Ling, A.C. Hopkinson, K.W.M. Siu, J. Phys. Chem. A 106 (2002) 8798;
(d) T. Shoeib, R.K. Milburn, G. Koyanagi, V.V. Lavrov, D.K. Bohme, K.W.M. Siu, A.C. Hopkinson, Int. J. Mass Spectrom. 201 (2000) 87;
(e) T. Shoeib, K.W.M. Siu, A.C. Hopkinson, J. Phys. Chem. A 106 (2002) 6121.
[39] T. Su, J. Chesnavich, J. Chem. Phys. 76 (1982) 5183.
[40] S.G. Lias, J.E. Bartmess, J.F. Liebman, J.L. Holmes, R.D. Levin, W.G. Mallard, in: W.G. Mallard, P.J. Linstrom (Eds.), Ion Energetics Data in NIST Chemistry WebBook, NIST Standard Reference Database Number 69, February 2000, National Institute of Standards and Technology, Gaithersburg, MD (http://webbook.nist.gov).
[41] A. Good, Trans. Faraday Soc. 67 (1971) 3495.
[42] R.C. Weast, M.J. Astle, CRC Handbook of Chemistry and Physics, 67th ed., CRC Press, Boca Raton, FL, 1986–1987.
[43] S.R. Langhoff, C.W. Bauschlicher, H. Partridge, M. Sodupe, J. Phys. Chem. 95 (1991) 10677.
[44] (a) D. Caraiman, G.K. Koyanagi, L.T. Scott, D.V. Preda, D.K. Bohme, J. Am. Chem. Soc. 123 (2001) 8573;
(b) P.M. Hierl, A.F. Ahrens, M.J. Henchman, A.A. Viggiano, J.F. Paulson, Int. J. Mass Spectrom. Ion Process. 81 (1987) 101.
[45] F. Meyer, Y.M. Chen, P.B. Armentrout, J. Am. Chem. Soc. 117 (1995) 4071.
[46] A.J. Lupinetti, V. Jonas, W. Thiel, S.H. Strauss, G. Frenking, Chem. Eur. J. 5 (1999) 2573.
[47] T. Magnera, D.E. David, D. Stulik, R.G. Orth, H.T. Jonkman, J. Michl, J. Am. Chem. Soc. 111 (1989) 5036.
[48] A.M. El-Nahas, N. Tajima, K. Hirao, J. Mol. Struct. 469 (1999) 201.
[49] P.M. Holland, A.W. Castleman, J. Chem. Phys. 76 (1982) 4195.
[50] D. Feller, E.D. Glendening, W.A. de Jong, J. Chem. Phys. 110 (1999) 1475.
[51] H. Deng, P. Kerbale, J. Phys. Chem. 102 (1998) 571.
[52] D. Walter, P.B. Armentrout, J. Am. Chem. Soc. 120 (1998) 3176.
[53] T. Shoeib, Silver–Ion Complexes Containing Amino Acids of Small Peptides: Theoretical and Experimental Studies, Ph.D. Dissertation, Department of Chemistry, York University, 2002.